Journal of
Composites Science

MDPI

Article

Determination of Quantum Capacitance of Niobium Nitrides Nb_2N and Nb_4N_3 for Supercapacitor Applications

Bharti [1,2], Gulzar Ahmed [1], Yogesh Kumar [3,*], Patrizia Bocchetta [4] and Shatendra Sharma [5]

1 Department of Physics, Mewar University, Gangrar, Chittorgarh 312901, India; bhartibaniwal@shivaji.du.ac.in (B.); gulzarahmed61@gmail.com (G.A.)
2 Department of Physics, Shivaji College, University of Delhi, New Delhi 110027, India
3 Department of Physics, ARSD College, University of Delhi, New Delhi 110021, India
4 Dipartimento di Ingegneria dell'Innovazione, Università del Salento, Via Monteroni, 73100 Lecce, Italy; patrizia.bocchetta@unisalento.it
5 School of Engineering and USIC, Jawaharlal Nehru University, New Delhi 110067, India; shatendra@gmail.com
* Correspondence: ykumar@arsd.du.ac.in; Tel.: +91-999-925-4014

Abstract: The density of states and quantum capacitance of pure and doped Nb_2N and Nb_4N_3 single-layer and multi-layer bulk structures are investigated using density functional theory calculations. The calculated value of quantum capacitance is quite high for pristine Nb_2N and decent for Nb_4N_3 structures. However for cobalt-doped unpolarized structures, significant increase in quantum capacitance at Fermi level is observed in the case of Nb_4N_3 as compared to minor increase in case of Nb_2N. These results show that pristine and doped Nb_2N and Nb_4N_3 can be preferred over graphene as the electrode material for supercapacitors. The spin and temperature dependences of quantum capacitance for these structures are also investigated.

Keywords: niobium nitride; electrode; supercapacitors; quantum capacitance

Citation: Bharti; Ahmed, G.; Kumar, Y.; Bocchetta, P.; Sharma, S. Determination of Quantum Capacitance of Niobium Nitrides Nb_2N and Nb_4N_3 for Supercapacitor Applications. *J. Compos. Sci.* **2021**, *5*, 85. https://doi.org/10.3390/jcs5030085

Academic Editor: Wei Yuan

Received: 4 March 2021
Accepted: 17 March 2021
Published: 20 March 2021

1. Introduction

Efficient and environment friendly energy conversion and storage is a challenge to researchers, with increasing demand for energy sources in electric (or hybrid) vehicles and portable electronic devices [1]. Supercapacitors are considered as viable devices for storing electrical energy because of their high energy and power densities and excellent discharging/charging performance [2,3]. Supercapacitor's energy density depends on the specific capacitance of the electrolyte-electrode system and the operating voltage [4]. The specific capacitance of an electrode in supercapacitor is a resultant of two capacitances, namely EDLC capacitance (C_{EDL}) and Quantum capacitance (QC), as represented by Equation (1) [5–7].

$$\frac{1}{C} = \frac{1}{QC} + \frac{1}{C_{EDL}}. \quad (1)$$

It is clear from the above equation that a low value of quantum capacitance can significantly decrease the total electrode capacitance. Therefore, apart from looking for advanced electrolytes, finding electrode materials with a high QC is a good way to increase the capacitance.

Carbon, metal oxides and conducting polymers are the most used material for supercapacitor electrodes [3,8–10]. However, conducting polymers and metal oxide electrodes exhibit poor electrochemical stability and electrical conductivity, whereas carbon electrodes suffer from poor capacitance. The graphene has been widely investigated for supercapacitor electrodes, because of its large specific surface area and electronic properties, but graphene also has low capacitance performance near Fermi level [6,11,12].

In search for better options, transition metal nitrides are explored as supercapacitor electrodes. These nitrides exhibit good chemical stability along with fair conductivity. They

are cost effective and have excellent electrochemical property which makes them suitable material for supercapacitor electrodes [13,14]. Transition metal nitrides, like vanadium nitride, titanium nitride, tungsten nitride etc., have already been investigated [15–20] as electrode materials. Among them, vanadium nitride is reported to have quite a high value (1340 F g^{-1}) of capacitance [15]. Different nanostructures of titanium nitride are prepared [21–23] to see their effectiveness as high energy supercapacitor electrodes. Many studies have been done regarding the fabrication of niobium nitrides and their superconducting properties. Experimental studies have already reported superconductivity in polycrystalline hexagonal ε-NbN [24] and in the tetragonal phases of both Nb_4N_3 and Nb_4N_5 with long-range-ordered arrangement of vacancies [25]. Nanowires and nanoribbons of Nb_4N_5 and Nb_5N_6 have also been fabricated and studied for their superconducting properties [26]. Researchers have used porous NbN as anode material and activated carbon as the cathode for a Li-ion hybrid capacitor LIHC [27]. The device has a wide potential window and exhibits a high energy and power density. Experimental study has been done using niobium nitride electrodes for hybrid supercapacitors as well. Niobium titanium nitride TiNbN is studied as supercapacitor electrode material [28] and a high specific capacitance value of up to 59.3 mF cm^{-2} at 1.0 mA cm^{-2} is achieved. The study has opened up the possibility of fabrication of all nitride-based asymmetric supercapacitors. In another study, niobium nitride Nb_4N_5 is explored to be an excellent capacitive material for the first time with an areal capacitance of 225.8 mF cm^{-2} [29]. Faradaic pseudo capacitance is confirmed by the mechanistic studies, deriving from the proton incorporation/chemisorption reaction owing to the copious +5 valence Nb ions in Nb_4N_5 [29]. Such studies prove the importance of exploring niobium nitride for supercapacitor applications.

Despite several reports on niobium nitrides, not much work is reported for their quantum capacitance. A thorough theoretical investigation on the QC of several structures of niobium nitride is required to assess their potential as supercapacitor electrode. The present work is further important as Nb_2N and Nb_4N_3 also satisfy the theoretical definition of MXenes. MXenes, a new class of two-dimensional materials, are produced from the ternary layered compounds [30]. MXene sheets [31] are a family of transition metal nitrides or carbides. These provide a substitute for graphene electrodes. These MXenes are synthesized by using hydrofluoric acid for exfoliation of "A" elements from their crystals known as MAX [32,33]. The "A" in MAX generally represents IV A or III A element (Si, Al, Ga etc.). The representative formula of MXene is $M_{m+1}X_m$ (m = 1, 2, 3 and so on), where "M" is an early transition metal like Ti, Mo, V, Cr, Zr, Hf, Nb and Ta and "X" is nitrogen or/and carbon [34–36]. MXenes are gaining attention due to their novel electronic and physical properties [37] and excellent mechanical flexibility [38,39]. MXenes with many layers generally exhibit better conductivity due to availability of more channels for transport of electrons, but the details in the impact of multilayers should be investigated individually. MXenes have been demonstrated to be thermally, chemically and mechanically stable and resistant to light radiation damage [40–43]. Due to these features, MXenes are being considered as a good option for a wide range of applications [38], including catalysis [44], energy storage [45], mano electronics [46–48], rechargeable batteries [49] and modern electronic devices [50]. Many investigations related to MXenes are focused on their applications in metal-ion batteries [51–54]. Few studies done to explore Mxenes for their supercapacitor applications have mainly explored Titanium-based MXenes [55,56]. No experimental work has been reported on niobium nitride MXene.

In this paper, for the first time, the QC of Nb_2N and Nb_4N_3 structures are determined using DFT calculations for supercapacitor applications. Effect of doping on quantum capacitance of these niobium nitride structures is also investigated. In our work, cobalt is used as dopant because of a recent experimental study [57] where the cobalt doping has shown a rise in capacity of niobium nitride.

Quantum capacitance values obtained are compared with that of graphene. Results of our calculation indicate that the limitation of low quantum capacitance graphene electrodes can be overcome by using Nb_2N and Nb_4N_3-based electrodes. More significantly, our

calculations indicate that the pristine or doped niobium nitrides exhibit very high values for QC at both the positive and negative electrodes. The dependence of quantum capacitance on number of molecular layers, spin and temperature is also investigated. The method of calculation and results are discussed in the following sections.

2. Materials and Methods

The DFT calculations for density of states were performed using the Atomistix Toolkit (ATK) package from QuantumWise (now known as Synopsys). The generalized gradient approximation (GGA) with the PBE functional was used to describe the exchange correlation energy [58]. The norm-conserving pseudopotential generated with the Fritz-Haber Institute FHI code was selected along with double zeta polarized basis set. The plane-wave energy cut off was kept at 540 eV, with Monkhorst-pack k-point grid meshes sampled at $12 \times 12 \times 1$. The crystal structures of Nb_2N and Nb_4N_3 were built using the crystal builder, as shown in Figure 1. The crystal parameters used for the computation are given in Table 1.

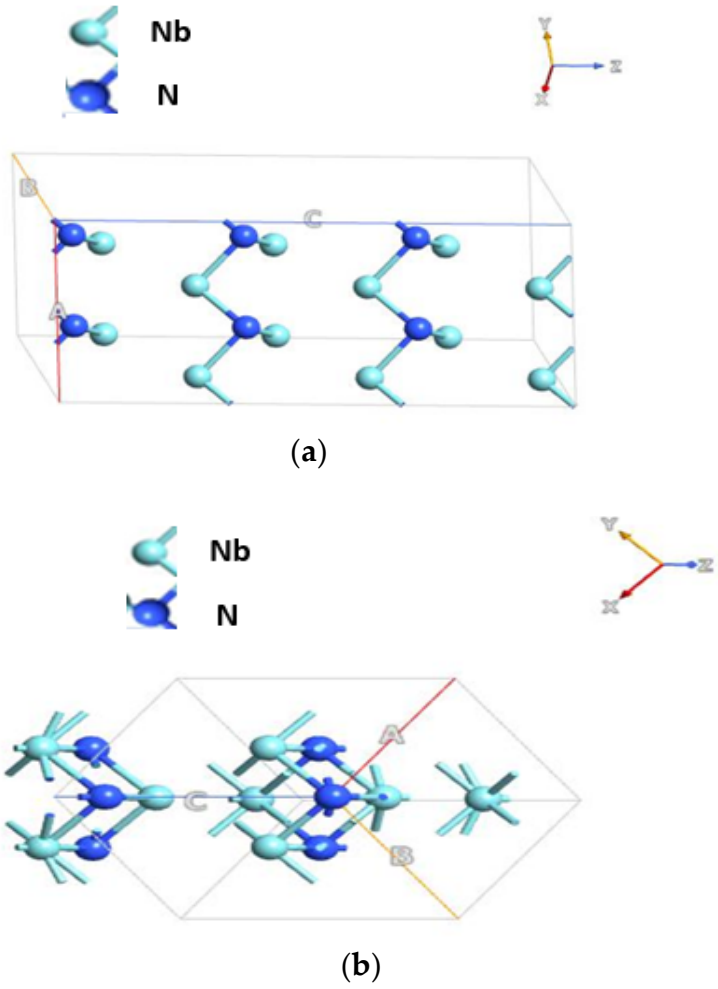

Figure 1. Chemical structures of pristine niobium nitride: (**a**) Nb_2N; (**b**) Nb_4N_3.

Table 1. Crystal parameters used for calculations.

Material	Crystal Structure	Space Group	Angles
Nb_2N	Hexagonal	6, Pm	$\alpha = \beta = 90°, \gamma = 120°$
Nb_4N_3	Body-centered tetragonal	8, Cm	$\alpha = \beta = \gamma = 90°$

Both structures of niobium nitride were doped (added) with 2 atoms of cobalt to investigate the doping effect on quantum capacitance, as shown in Figure 2. Geometry optimization for doped structures was done using the QuasiNewton optimizer method of the ATK package, with maximum force and stress 0.05 eV/Å and 0.05 eV/Å^3, respectively. The density of states was computed for the geometry optimized structures of doped Nb_2N and Nb_4N_3.

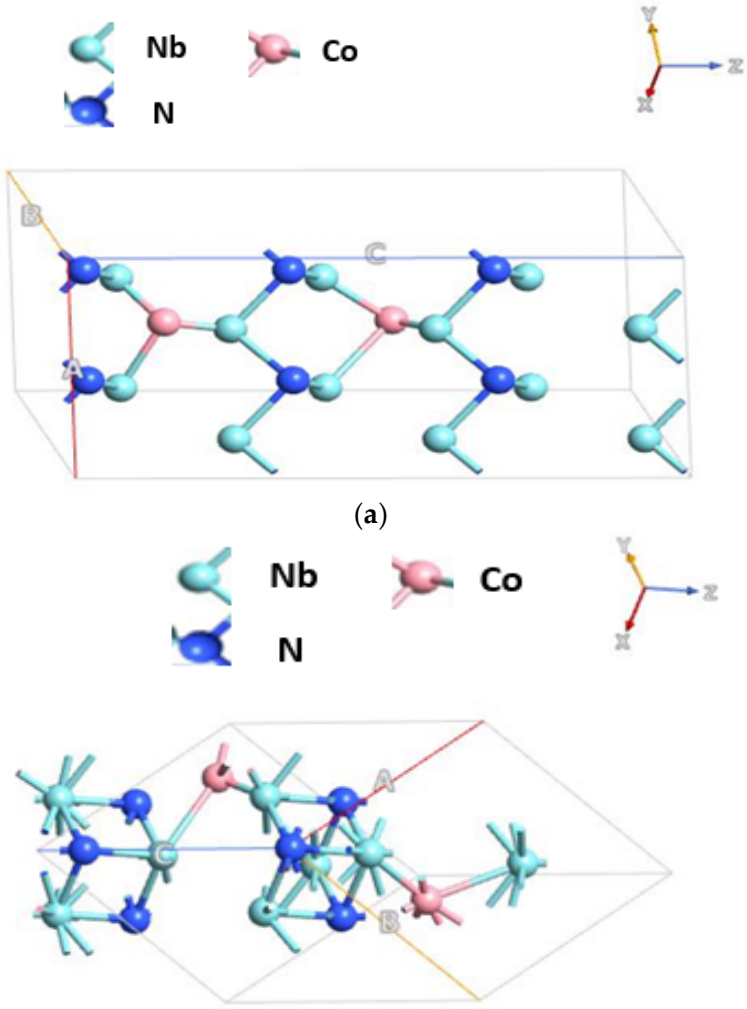

Figure 2. Chemical structures of doped niobium nitride: (**a**) Nb_2N-2Co; (**b**) Nb_4N_3-2Co.

Quantum capacitance of electrodes was calculated using the computed density of states (DOSs). If ϕ is the operating voltage and Q is the surface charge on niobium nitride, then, from density of state DOS (E), we can find quantum capacitance using Equations (2)–(4) [59,60]:

$$Q = e\int_{-\infty}^{+\infty} DOS(E)[f(E) - f(E - e\phi)]\, dE \tag{2}$$

$$f(E) = \frac{1}{1 + \exp\left(\frac{E}{kT}\right)}, \tag{3}$$

where e is the electronic charge, $f(E)$ is the Fermi-Dirac distribution function and E is the energy w.r.t the Fermi energy.

By definition, one can obtain quantum capacitance by differentiating Q w.r.t ϕ, that is,

$$QC = \frac{dQ}{d\phi} = e^2 \int_{-\infty}^{+\infty} DOS(E) \times \frac{sech^2\left(\frac{E-e\phi}{2kT}\right)}{4kT} dE. \quad (4)$$

Doping impacts the electronic structure of materials, thus changing the density of states. Due to these changes, the quantum capacitance gets modified [61]. The variation in the electronic DOS and corresponding change in the value of quantum capacitance were studied for different operating voltages for pristine and doped structures.

The dependence of quantum capacitance on spin, number of layers and temperature was also investigated.

3. Results and Discussion

3.1. Unpolarised Pristine Structures

Density of states are determined to calculate the quantum capacitance of pristine Nb_2N and Nb_4N_3 using the DFT method without spin. The calculated density of states are shown in Figure 3a,b, respectively.

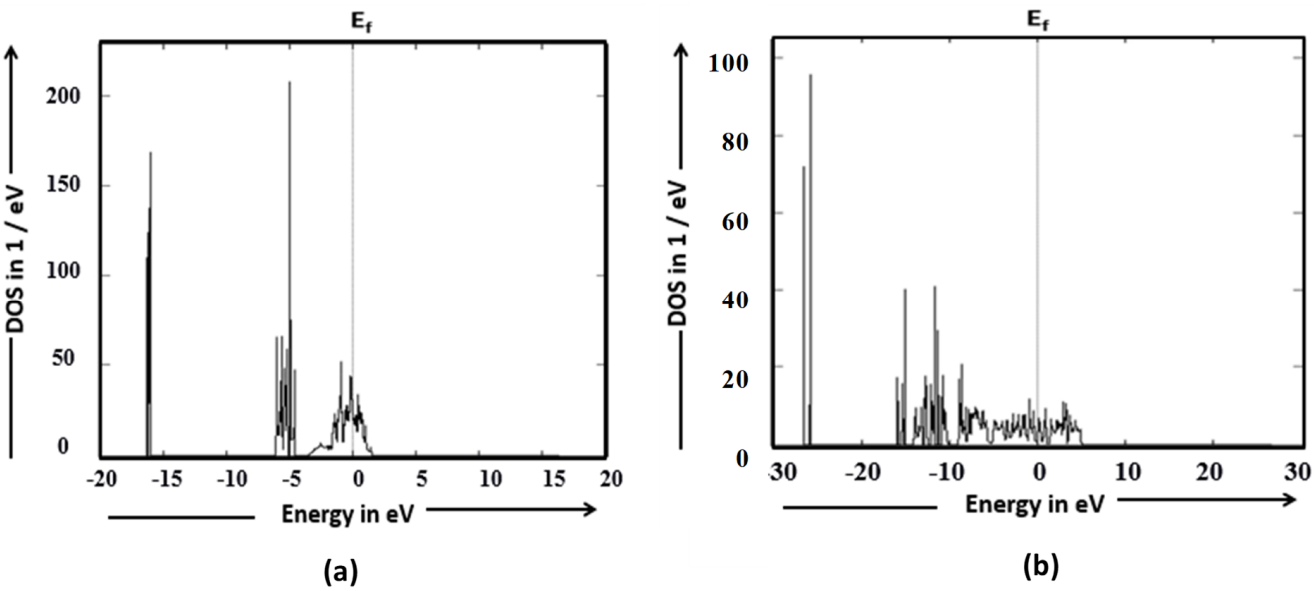

Figure 3. The density of states (DOSs) for (**a**) Nb_2N and (**b**) Nb_4N_3.

In Figure 3a, pronounced peaks in DOS are observed for Nb_2N at and near Fermi level (in the range of interest). The peaks of the density of states close to the Fermi level are expected to make a major contribution to the QC as per Equation (4). For Nb_2N, the calculations show very high values of quantum capacitance at different bias voltages, the highest being 1196.28 μF cm^{-2} at −1 V, as shown in Figure 4. However, for Nb_4N_3, the peaks are not that pronounced (Figure 3b) but are high enough to give a quantum capacitance value of 174.86 μF cm^{-2}, near Fermi level. These values obtained for Nb_4N_3 at different bias voltages around Fermi level are lower than that of Nb_2N but are higher than that of graphene, the most widely used electrode material for supercapacitor. It is well known that the quantum capacitance of pristine graphene electrode is very low due to its low density of state (DOS) near the Fermi level. The QC of pristine graphene has been investigated experimentally and theoretically [6,11,12,62], and it was found that the presence of Dirac point in DOS at Fermi level in the case of graphene results in extremely low values of quantum capacitance (in the range of 4~6 μF cm^{-2}).

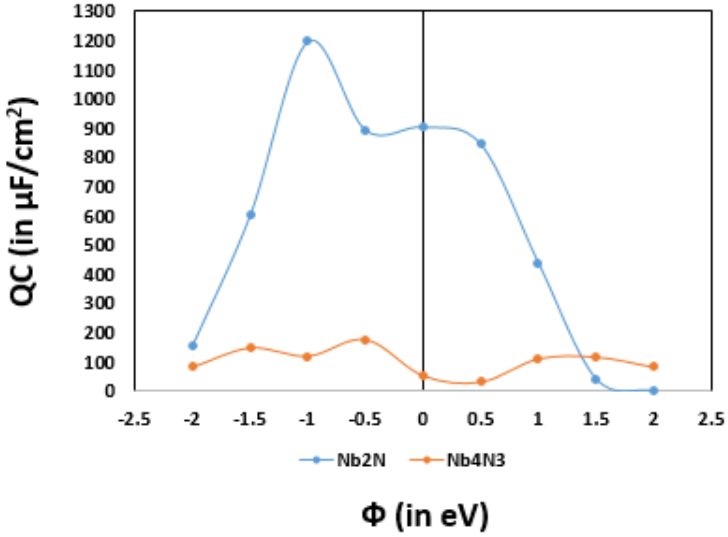

Figure 4. Variation in quantum capacitance (QC) for pristine unpolarized niobium nitride structures under bias voltage.

The QC values obtained for both structures at different bias voltages are compared in Figure 4. It is found that quantum capacitance of Nb_2N remains higher than Nb_4N_3 for most of the bias voltage range. Although QC values for Nb_4N_3 are lower than Nb_2N, they are still high enough (Figure 4) for use as electrode material for supercapacitors.

3.2. Effect of Number of Layers

In order to investigate the impact of increasing molecular layers in the crystal structure, these calculations were repeated for up to three layers. The values of quantum capacitance are found to increase with increase in number of layers for both Nb_2N and Nb_4N_3, as shown in Figure 5a,b, respectively.

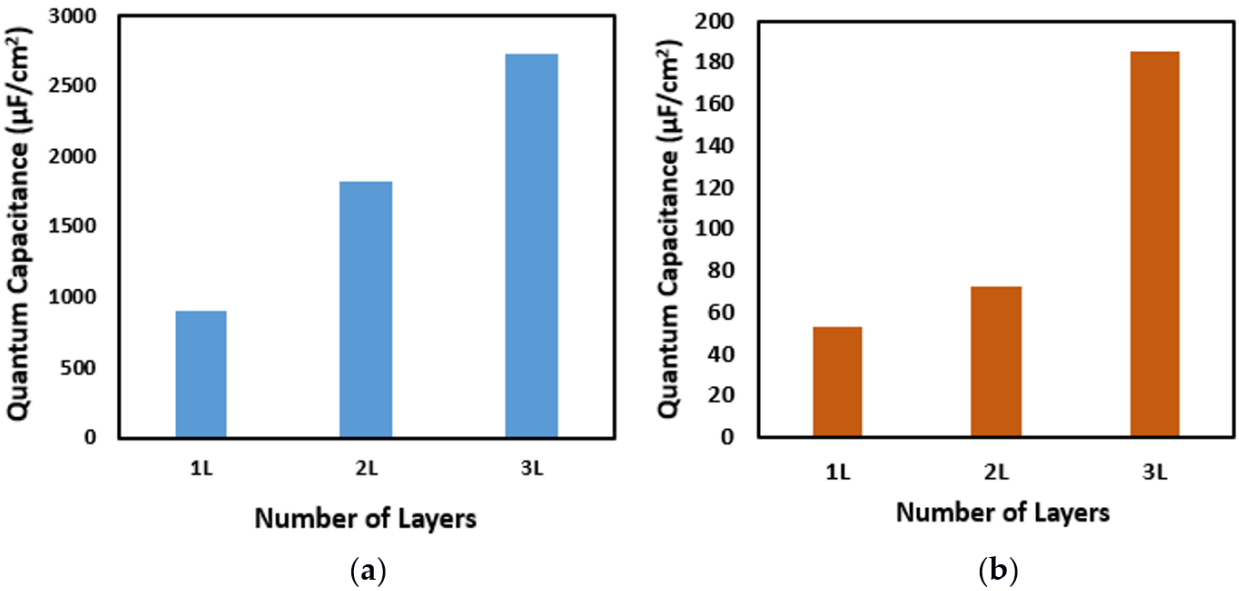

Figure 5. Variation of quantum capacitance QC with number of layers for (**a**) Nb_2N and (**b**) Nb_4N_3.

A similar trend of increase in QC with increase in layers is also reported in the case of graphene [59].

3.3. Effect of Cobalt Doping

The impact of cobalt doping on density of states and, subsequently, on quantum capacitance of both structures of niobium nitride was investigated. Comparison of density of states of pristine and doped structures of Nb_2N and Nb_4N_3 are shown in Figure 6. The density of states for pristine Nb_2N and Nb_4N_3 are increased at Fermi level when they are doped with two atoms of cobalt, as shown in Figure 6a,b. This rise in DOS at Fermi level is mainly due to the contribution in DOS from the 3d electrons of cobalt dopant. Little contribution to the rise in DOS also comes from the electrons of the 4s subshell of cobalt. This increase in the density of states contributes to the increase in QC.

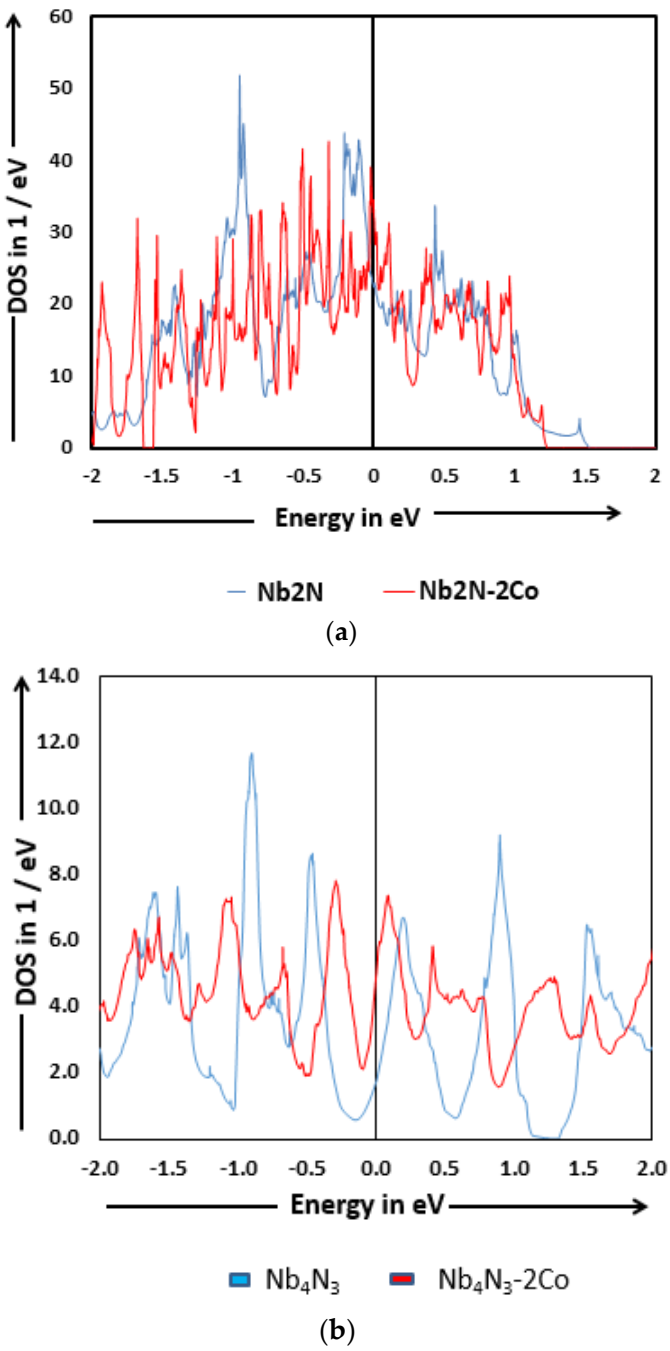

Figure 6. Comparison of the density of states at and near Fermi Level of (**a**) Nb_2N and Nb_2N-2Co; (**b**) Nb_4N_3 and Nb_4N_3-2Co.

The calculated quantum capacitance values for unpolarized Nb_4N_3-2Co and Nb_2N-2Co depicts a rise in QC in comparison to their pristine counterparts at Fermi level, as shown in Figure 7. At Fermi level, rise in QC by factors of 2.5 and 1.2 is observed in doped Nb_4N_3 and Nb_2N, respectively. The increase is in agreement to the increase in the total density of states of Nb_4N_3 and Nb_2N after doping at Fermi level, which is clearly visible in Figure 6. For cobalt-doped Nb_4N_3, the QC is in the range of 65.85 to 135.2 μF cm^{-2} in the area of interest, as shown in Figure 7a. It is found that the low values of quantum capacitance at Fermi level obtained in the case of pristine Nb_4N_3 can be increased when doping with cobalt.

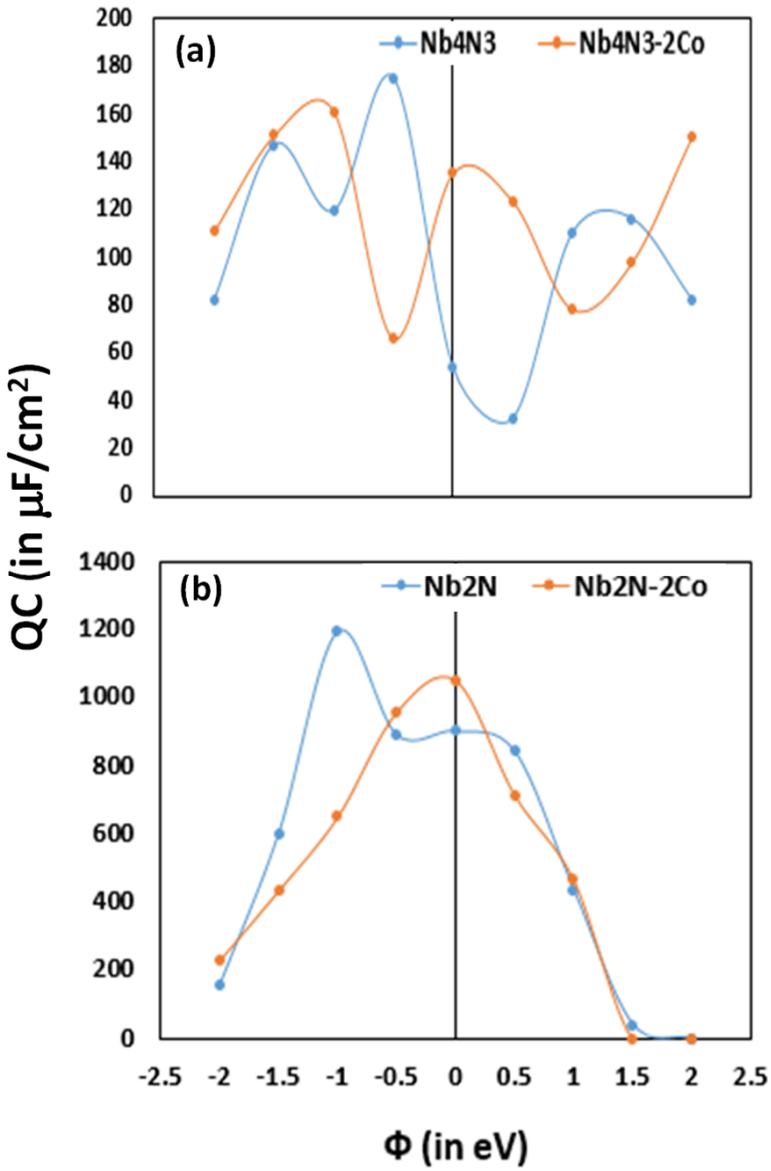

Figure 7. Comparison of calculated QC at different bias voltages for pristine and doped unpolarized structures. (**a**) Nb_4N_3 and Nb_4N_3-2Co; (**b**) Nb_2N and Nb_2N-2Co.

However, doping with cobalt shows only a slight increase in the QC at Fermi level in the case of Nb_2N, reaching to value 1052.2 μF cm^{-2} (Figure 7b). At all other bias voltages, pristine Nb_2N shows similar or slightly higher values for QC than doped Nb_2N. The variation in QC of pristine Nb_2N after doping with cobalt can be completely understood by comparing the DOS of pristine and doped structures of Nb_2N. As shown in Figure 6a, the DOS for doped Nb_2N is slightly higher than that of its pristine counterpart, resulting in

a slight increase in QC at Fermi level. For positive energies, the DOSs are almost similar for both pristine and doped structures, hence showing similar values of QC for positive bias voltages. The fall in QC in doped Nb_2N at −1 V is attributed to a fall in its DOS near −1 eV as shown in Figure 6a.

3.4. Effect of Spin on Pristine and Doped Structures

The spin polarized calculations were also done on pristine and doped Nb_2N and Nb_4N_3 structures. The comparison of density of states near Fermi level and QC value obtained at Fermi level of pure and doped structures are plotted and given in Figures 8 and 9.

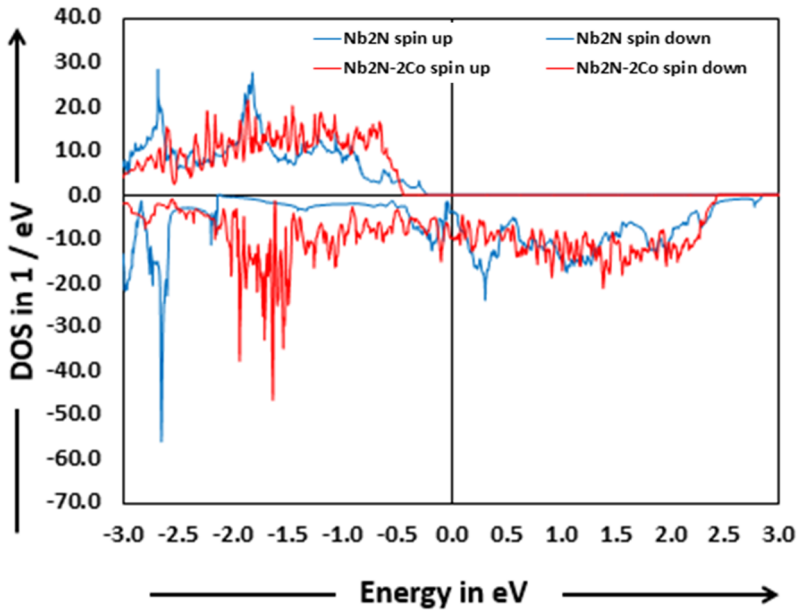

(**a**)

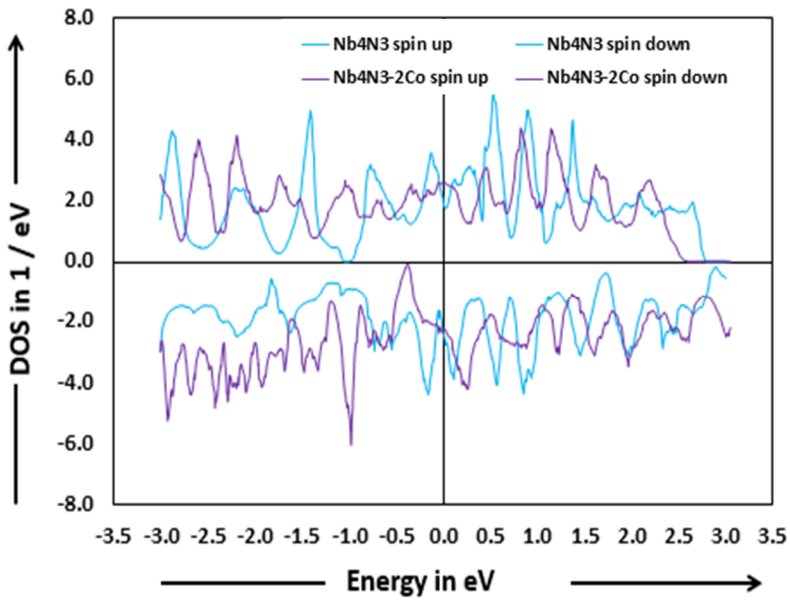

(**b**)

Figure 8. Comparison of the density of states of spin polarized (**a**) Nb_2N and Nb_2N-2Co and (**b**)Nb_4N_3 and Nb_4N_3-2Co.

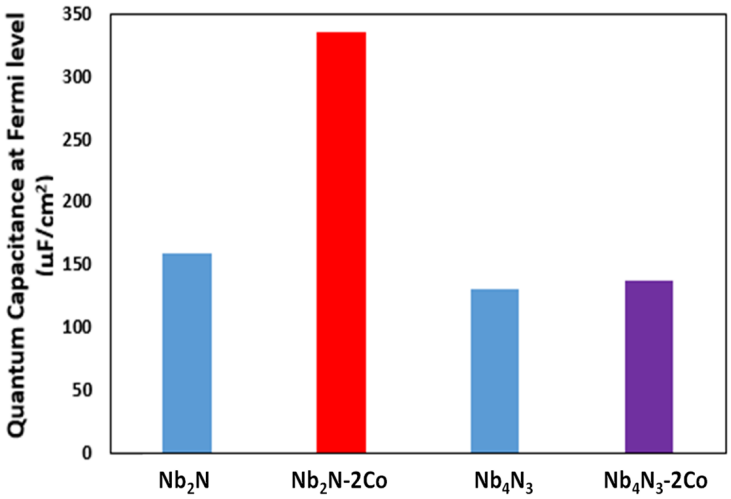

Figure 9. Comparison of calculated QC for pristine and doped polarized structures at Fermi level.

In case of Nb_2N, there is an increase in DOS at and near Fermi level after cobalt doping, as shown in Figure 8a. The increase is due to the contribution of 4d and 5s electrons of cobalt. This increase doubles the QC value at Fermi level for doped Nb_2N as compared to its pristine counterpart, as shown in Figure 9 (Histo). Whereas, in the case of Nb_4N_3, not much increase is seen in DOS (Figure 8b) at Fermi level after doping, resulting in a very small increase in QC at Fermi Level, as shown in Figure 9.

3.5. Effect of Temperature on Quantum Capacitance

Calculations for quantum capacitance were done at three different temperatures (i.e., 233, 300 and 353 K). No significant change was noted in the DOSs profile. For pristine unpolarized Nb_2N and Nb_4N_3, a change in temperature from 233 to 353 K increases the QC at Fermi level slightly from 878.3 to 921 μF cm^{-2} and 51.72 to 54.34 μF cm^{-2}, respectively. In case of cobalt-doped structures of Nb_2N and Nb_4N_3, the change observed is 5% and 8%, respectively. The slight change in the QC values is mainly due to the Fermi Dirac distribution function present in the equations used for calculating quantum capacitance. Similar studies done for graphene at different temperature ranges have also shown negligible impact of temperature on QC of graphene [63].

4. Conclusions

DFT calculations are performed to investigate the quantum capacitance of niobium nitrides Nb_2N and Nb_4N_3 for their possible use as supercapacitor electrode materials. Out of the two pristine structures investigated, Nb_2N is the most promising candidate for fabrication of supercapacitor electrodes, with theoretical QC reaching up to 1196.28 μF cm^{-2} at −1 V for unpolarized Nb_2N. Even for positive bias voltage range, quantum capacitance values for Nb_2N exceeds the QC values of Nb_4N_3, reaching a value of 844.8 μF cm^{-2} at 0.5 V. Impact of increase in layers on QC is also investigated and it is found that the quantum capacitance increases with increase in layers for both pristine niobium nitrides.

A viable method is proposed to enhance the quantum capacitance of niobium nitride using suitable dopant. The results show that the value of QC of pristine structures at Fermi level can be further increased by doping with cobalt. The maximum value of quantum capacitance in doped structures is obtained for unpolarized doped Nb_2N (1052.2 μF cm^{-2}) at Fermi level. The impact of polarization is also studied on both pure and doped structures and a substantial increase is seen in QC at Fermi level for Nb_2N after doping with cobalt. The calculations done for pristine and cobalt-doped Nb_2N and Nb_4N_3 structures show no significant temperature dependence of DOS and a slight change in quantum capacitance with temperature.

Author Contributions: B. and S.S.—Modelling, simulation, computations and analysis of results, preparation of manuscript and figures; Y.K. and G.A.—Conceptualization, analysis, and overall supervision; P.B.—Critical analysis and presentation of results. All authors have read and agreed to the published version of the manuscript.

Funding: This research received no external funding.

Acknowledgments: Authors acknowledge the help from University Science and Instrumentation Centre, USIC, JNU, Delhi for providing the computing resources.

Conflicts of Interest: The authors declare that there are no conflicts of interest regarding the publication of this paper.

References

1. Hughes, Z.E.; Walsh, T.R. Computational chemistry for graphene-based energy applications: Progress and challenges. *Nanoscale* **2015**, *7*, 6883. [CrossRef] [PubMed]
2. Ponnamma, D.; Vijayan, P.; Al-Maadeed, M.A.A. 3D architectures of titania nanotubes and graphene with efficient nanosynergy for supercapacitors. *Mater. Des.* **2017**, *117*, 203. [CrossRef]
3. Wang, G.; Zhang, L.; Zhang, J. A review of electrode materials for electrochemical supercapacitors. *Chem. Soc. Rev.* **2012**, *41*, 797. [CrossRef]
4. Paek, E.; Pak, A.J.; Kweon, K.E.; Hwang, G.S. On the origin of the enhanced supercapacitor performance of nitrogen-doped graphene. *J. Phys. Chem. C* **2013**, *117*, 5610. [CrossRef]
5. Pak, A.J.; Paek, E.; Hwang, G.S. Relative contributions of quantum and double layer capacitance to the supercapacitor performance of carbon nanotubes in an ionic liquid. *Phys. Chem. Chem. Phys.* **2013**, *15*, 19741. [CrossRef] [PubMed]
6. Stoller, M.D.; Magnuson, C.W.; Zhu, Y.; Murali, S.; Suk, J.W.; Piner, R.; Ruoff, R.S. Interfacial capacitance of single layer graphene. *Energy Environ. Sci.* **2011**, *4*, 4685. [CrossRef]
7. Xia, J.; Chen, F.; Li, J.; Tao, N. Measurement of the quantum capacitance of graphene. *Nat. Nanotechnol.* **2009**, *4*, 505. [CrossRef]
8. Zhao, X.; Sanchez, B.M.; Dobson, P.J.; Grant, P.S. High-performance symmetric electrochemical capacitor based on graphene foam and nanostructured manganese oxide. *Nanoscale* **2011**, *3*, 839. [CrossRef]
9. Simon, P.; Gogotsi, Y. Materials for electrochemical capacitors. *Nat. Mater.* **2008**, *7*, 845. [CrossRef] [PubMed]
10. Zhang, L.L.; Zhao, X. Carbon-based materials as supercapacitor electrodes. *Chem. Soc. Rev.* **2009**, *38*, 2520. [CrossRef]
11. John, D.L.; Castro, L.C.; Pulfrey, D.L. Quantum capacitance in nanoscale device modeling. *J. Appl. Phys.* **2004**, *96*, 5180. [CrossRef]
12. Paek, E.; Pak, A.J.; Hwang, G.S. A computational study of the interfacial structure and capacitance of graphene in [BMIM][PF_6] ionic liquid. *J. Electrochem. Soc.* **2013**, *160*. [CrossRef]
13. Dong, S.; Chen, X.; Zhang, X.; Cui, G. Nanostructured transition metal nitrides for energy storage and fuel cells. *Coord. Chem. Rev.* **2013**, *257*, 1946. [CrossRef]
14. Balogun, M.S.; Qiu, W.; Wang, W.; Fang, P.; Lu, X.; Tong, Y. Recent advances in metal nitrides as high-performance electrode materials for energy storage devices. *J. Mater. Chem. A* **2015**, *3*, 1364. [CrossRef]
15. Choi, D.; Blomgren, G.E.; Kumta, P.N. Fast and reversible surface redox reaction in nanocrystalline vanadium nitride supercapacitors. *Adv. Mater.* **2006**, *18*, 1178. [CrossRef]
16. Choi, D.; Kumta, P.N. Nanocrystalline TiN derived by a two-step halide approach for electrochemical capacitors. *J. Electrochem. Soc.* **2006**, *153*, A2298. [CrossRef]
17. Choi, D.; Kumta, P.N. Synthesis, structure, and electrochemical characterization of nanocrystalline tantalum and tungsten nitrides. *J. Am. Ceram. Soc.* **2007**, *90*, 3113. [CrossRef]
18. Choi, D.; Kumta, P.N. Synthesis and characterization of nanostructured niobium and molybdenum nitrides by a two-step transition metal halide approach. *J. Am. Ceram. Soc.* **2011**, *94*, 2371. [CrossRef]
19. Lu, X.; Wang, G.; Zhai, T.; Yu, M.; Xie, S.; Ling, Y.; Liang, C.; Tong, Y.; Li, Y. Stabilized TiN nanowire arrays for high-performance and flexible supercapacitors. *Nano Lett.* **2012**, *12*, 5376. [CrossRef]
20. Lu, X.; Yu, M.; Zhai, T.; Wang, G.; Xie, S.; Liu, T.; Liang, C.; Tong, Y.; Li, Y. High energy density asymmetric quasi-solid-state supercapacitor based on porous vanadium nitride nanowire anode. *Nano Lett.* **2013**, *13*, 2628. [CrossRef]
21. Xie, Y.; Wang, Y.; Du, H. Electrochemical capacitance performance of titanium nitride nanoarray. *Mater. Sci. Eng. B* **2013**, *178*, 1443. [CrossRef]
22. Dong, S.; Chen, X.; Gu, L.; Zhou, X.; Xu, H.; Wang, H.; Liu, Z.; Han, P.; Yao, J.; Wang, L. Facile preparation of mesoporous titanium nitride microspheres for electrochemical energy storage. *ACS Appl. Mater. Interfaces* **2011**, *3*, 93. [CrossRef] [PubMed]
23. Lu, X.; Liu, T.; Zhai, T.; Wang, G.; Yu, M.; Xie, S.; Ling, Y.; Liang, C.; Tong, Y.; Li, Y. Improving the cycling stability of metal-nitride supercapacitor electrodes with a thin carbon shell. *Adv. Energy Mater.* **2014**, *4*, 1300994. [CrossRef]
24. Zou, Y.; Qi, X.; Zhang, C.; Ma, S.; Zhang, W.; Li, Y.; Chen, T.; Wang, X.; Chen, Z.; Welch, D.; et al. Discovery of superconductivity in hard hexagonal ε-NbN. *Sci. Rep.* **2016**, *6*, 22330. [CrossRef] [PubMed]
25. Oya, G.-i.; Onodera, Y. Transition temperatures and crystal structures of single-crystal and polycrystalline NbN_X films. *J. Appl. Phys.* **1974**, *45*, 1389. [CrossRef]

26. Patel, U.; Avci, S.; Xiaoa, Z.L.; Hua, J.; Yu, S.H.; Ito, Y. Synthesis and superconducting properties of niobium nitride nanowires and nanoribbons. *Appl. Phys. Lett.* **2007**, *91*, 162508. [CrossRef]
27. Wang, P.; Wang, R.; Lang, J.; Zhang, X.; Chena, Z.; Yan, X. Porous niobium nitride as a capacitive anode material for advanced Li-ion hybrid capacitors with superior cycling stability. *J. Mater. Chem. A* **2016**, *4*, 9760. [CrossRef]
28. Wei, B.; Ming, F.; Liang, H.; Wenshen, H.; Wanga, Z. All nitride asymmetric supercapacitors of niobium titanium nitride-vanadium nitride. *J. Power Sour.* **2021**, *481*, 228842. [CrossRef]
29. Cui, H.; Zhu, G.; Liu, X.; Liu, F.; Xie, Y.; Yang, C.; Lin, T.-q.; Gu, H.; Huang, F. Niobium nitride Nb_4N_5 as a new high-performance electrode material for supercapacitors. *Adv. Sci.* **2015**, *2*, 1500126. [CrossRef]
30. Ng, V.M.H.; Huang, H.; Zhou, K.; Lee, P.S.; Que, W.; Xu, J.Z.; Kong, L.B. Recent progress in layered transition metal carbides and/or nitrides (MXenes) and their composites: Synthesis and applications. *J. Mater. Chem. A* **2017**, *5*, 3039. [CrossRef]
31. Barsoum, M.W. The $M_{N+1}AX_N$ phases: A new class of solids: Thermodynamically stable nanolaminates. *Prog. Solid State Chem.* **2000**, *28*, 201. [CrossRef]
32. Naguib, M.; Mashtalir, O.; Carle, J.; Presser, V.; Lu, J.; Hultman, L.; Gogotsi, Y.; Barsoum, M.W. Two-dimensional transition metal carbides. *ACS Nano* **2012**, *6*, 1322. [CrossRef]
33. Naguib, M.; Kurtoglu, M.; Presser, V.; Lu, J.; Niu, J.; Heon, M.; Hultman, L.; Gogotsi, Y.; Barsoum, M.W. Two-dimensional nanocrystals produced by exfoliation of Ti_3AlC_2. *Adv. Mater.* **2011**, *23*, 4248. [CrossRef]
34. Pang, J.; Mendes, R.G.; Bachmatiuk, A.; Zhao, L.; Ta, H.Q.; Liu, T.G.H.; Liu, Z.; Rummeli, M.H. Applications of 2D MXenes in energy conversion and storage systems. *Chem. Soc. Rev.* **2019**, *48*, 72. [CrossRef] [PubMed]
35. Gogotsi, Y.; Anasori, B. The rise of MXenes. *ACS Nano* **2019**, *13*, 8491. [CrossRef] [PubMed]
36. Khazaei, M.; Mishra, A.; Venkataramanan, N.S.; Singh, A.K.; Yunoki, S. Recent advances in MXenes: From fundamentals to applications. *Curr. Opin. Solid State Mater. Sci.* **2019**, *23*, 164. [CrossRef]
37. Khazaei, M.; Arai, M.; Sasaki, T.; Chung, C.Y.; Venkataramanan, N.S.; Estili, M.; Sakka, Y.; Kawazoe, Y. Novel electronic and magnetic properties of two-dimensional transition metal carbides and nitrides. *Adv. Funct. Mater.* **2013**, *23*, 2185. [CrossRef]
38. Ling, Z.; Ren, C.E.; Zhao, M.Q.; Yang, J.; Giammarco, J.M.; Qiu, J.; Barsoum, M.W.; Gogotsi, Y. Flexible and conductive MXene films and nanocomposites with high capacitance. *Proc. Nat. Acad. Sci. USA* **2014**, *111*, 16676. [CrossRef]
39. Guo, Z.L.; Zhou, J.; Si, C.; Sun, Z.M. Flexible two-dimensional Tin+1Cn (n = 1, 2 and 3) and their functionalized MXenes predicted by density functional theories. *Phys. Chem. Chem. Phys.* **2015**, *17*, 15348. [CrossRef]
40. Naguib, M.; Mochalin, V.N.; Barsoum, M.W.; Gogotsi, Y. 25th anniversary article: MXenes: A new family of two-dimensional materials. *Adv. Mater.* **2014**, *26*, 992. [CrossRef]
41. Li, Z.; Wang, L.; Sun, D.; Zhang, Y.; Liu, B.; Hu, Q.; Zhou, A. Synthesis and thermal stability of two-dimensional carbide MXene Ti_3C_2. *Mater. Sci. Eng. B* **2015**, *191*, 33. [CrossRef]
42. Khazaei, M.; Ranjbar, A.; Arai, M.; Sasaki, T.; Yunoki, S. Electronic properties and applications of MXenes: A theoretical review. *J. Mater. Chem. C* **2017**, *5*, 2488. [CrossRef]
43. Chen, C.; Ji, X.; Xu, K.; Zhang, B.; Miao, L.; Jiang, J. Prediction of T- and H-phase two dimensional transition-metal carbides/nitrides and their semiconducting-metallic phase transition. *Chem. Phys. Chem.* **2017**, *18*, 1897. [CrossRef]
44. Liu, H.; Duan, C.; Yang, C.; Shen, W.; Wang, F.; Zhu, Z. A novel nitrite biosensor based on the direct electrochemistry of hemoglobin immobilized on MXene-Ti_3C_2. *Sensor. Actuators B Chem.* **2015**, *218*, 60. [CrossRef]
45. Anasori, B.; Lukatskaya, M.R.; Gogotsi, Y. 2D metal carbides and nitrides (MXenes) for energy storage. *Nat. Rev. Mater.* **2017**, *2*, 16098. [CrossRef]
46. Zhou, Y.; Luo, K.; Zha, X.; Liu, Z.; Bai, X.; Huang, Q.; Guo, Z.; Lin, C.; Du, S. Electronic and transport properties of Ti_2Co_2 MXene nanoribbons. *J. Phys. Chem. C* **2016**, *120*, 17143. [CrossRef]
47. Mortazavi, B.; Shahrokhi, M.; Makaremi, M.; Rabczuk, T. Anisotropic mechanical and optical response and negative Poisson's ratio in Mo_2C nanomembranes revealed by first-principles simulations. *Nanotechnology* **2017**, *28*, 115705. [CrossRef]
48. Lipatov, A.; Alhabeb, M.; Lukatskaya, M.R.; Boson, A.; Gogotsi, Y.; Sinitskii, A. Efect of synthesis on quality, electronic properties and environmental stability of individual monolayer Ti_3C_2 MXene fakes. *Adv. Electron. Mater.* **2016**, *2*, 1600255. [CrossRef]
49. Mortazavi, B.; Shahrokhi, M.; Makaremi, M.; Rabczuk, T. Theoretical realization of Mo_2P; a novel stable 2D material with superionic conductivity and attractive optical properties. *Appl. Mater. Today* **2017**, *9*, 292. [CrossRef]
50. Zhao, P.; Jin, H.; Lv, X.; Huang, B.; Ma, Y.; Dai, Y. Modifed MXene: Promising electrode materials for constructing ohmic contacts with MoS_2 for electronic device applications. *Phys. Chem. Chem. Phys.* **2018**, *20*, 16551. [CrossRef]
51. Eames, C.; Islam, M.S. Ion intercalation into two-dimensional transition-metal car-bides: Global screening for new high-capacity battery materials. *J. Am. Chem. Soc.* **2014**, *136*, 16270. [CrossRef]
52. Naguib, M.; Come, J.; Dyatkin, B.; Presser, V.; Taberna, P.L.; Simon, P.; Barsoum, M.W.; Gogotsi, Y. MXene: A promising transition metal carbide anode for lithium-ion batteries. *Electrochem. Commun.* **2012**, *16*, 61. [CrossRef]
53. Yu, Y.X. Prediction of mobility, enhanced storage capacity, and volume change during sodiation on interlayer-expanded functionalized Ti_3C_2 MXene anode materials for sodium-ion batteries. *J. Phys. Chem. C* **2016**, *120*, 5288. [CrossRef]
54. Liang, X.; Garsuch, A.; Nazar, L.F. Sulfur cathodes based on conductive MXene nanosheets for high performance lithium-sulfur batteries. *Angew. Chem. Int. Ed.* **2015**, *54*, 3907. [CrossRef] [PubMed]

55. Lukatskaya, M.R.; Mashtalir, O.; Ren, C.E.; Dall'Agnese, Y.; Rozier, P.; Taberna, P.L.; Naguib, M.; Simon, P.; Barsoum, M.W.; Gogotsi, Y. Cation intercalation and high volumetric capacitance of two-dimensional titanium carbide. *Science* **2013**, *341*, 1502. [CrossRef]
56. Hu, M.; Li, Z.J.; Hu, T.; Zhang, C.; Wu, Z.; Wang, X.H. Self-assembled $Ti_3C_2T_X$ MXene film with high gravimetric capacitance. *Chem. Commun.* **2015**, *51*, 13531. [CrossRef]
57. Ge, W.; Wang, L.; Li, C.; Wang, C.; Wang, D.; Qian, Y.; Xu, L. Conductive cobalt doped niobium nitride porous spheres as efficient polysulfide convertor for advanced lithium-sulfur batteries. *J. Mater. Chem. A* **2020**, *8*, 6276. [CrossRef]
58. Perdew, J.P.; Burke, K.; Ernzerhof, M. Generalized gradient approximation made simple. *Phys. Rev. Lett.* **1996**, *77*, 3865. [CrossRef]
59. Zhan, C.; Neal, J.; Wu, J.; Jiang, D.E. Quantum effects on the capacitance of graphene-based electrodes. *J. Phys. Chem. C* **2015**, *119*, 22297. [CrossRef]
60. Yang, G.M.; Zhang, H.Z.; Fan, X.F.; Zheng, W.T. Density functional theory calculations for the quantum capacitance performance of graphene-based electrode material. *J. Phys. Chem. C* **2015**, *119*, 6464. [CrossRef]
61. Elias, D.C.; Gorbachev, R.V.; Mayorov, A.S.; Morozov, S.V.; Zhukov, A.A.; Blake, P.; Ponomarenko, L.A.; Grigorieva, I.V.; Novoselov, K.S.; Guinea, F.; et al. Dirac cones reshaped by interaction effects in suspended graphene. *Nat. Phys.* **2011**, *7*, 701. [CrossRef]
62. Frackowiak, E. Carbon materials for supercapacitor application. *Phys. Chem. Chem. Phys.* **2007**, *9*, 1774. [CrossRef] [PubMed]
63. Vatamanu, J.; Ni, X.; Liu, F.; Bedrov, D. Tailoring graphene-based electrodes from semiconducting to metallic to increase the energy density in supercapacitors. *Nanotechnology* **2015**, *26*, 46. [CrossRef] [PubMed]